

Supporting information for

Template Orienting One-Dimensional Schiff-Base Polymer: towards Flexible Nitrogen-enriched Carbonaceous Electrodes with Ultrahigh Electrochemical Capacity

Zhichang Xiao,^{*a} Junwei Han,^c Haiyong He,^d Xinghao Zhang,^b Jing Xiao,^c Daliang Han,^c Debin Kong,^{*c} Bin Wang,^b Quan-Hong Yang,^c and Linjie Zhi ^{*b}

^aDepartment of Chemistry, College of Science, Hebei Agricultural University, Baoding 071001, P. R. China

^bCAS Key Laboratory of Nanosystem and Hierarchical Fabrication, CAS Center for Excellence in Nanoscience, National Center for Nanoscience and Technology, Beijing 100190, P. R. China

^cNanoyang Group, State Key Laboratory of Chemical Engineering, School of Chemical Engineering and Technology, Collaborative Innovation Center of Chemical Science and Engineering (Tianjin), Tianjin University, Tianjin 300350, P. R. China

^dNingbo Institute of Materials Technology and Engineering, Chinese Academy of Sciences, Ningbo, 315201, P. R. China

^eCollege of New Energy, China University of Petroleum (East China), Qingdao, P. R. China.

*Corresponding author. E-mail: zhilj@nanoctr.cn (Linjie Zhi); kongdb@upc.edu.cn (Debin Kong); xiaozhichangcnu@sina.cn (Zhichang Xiao).

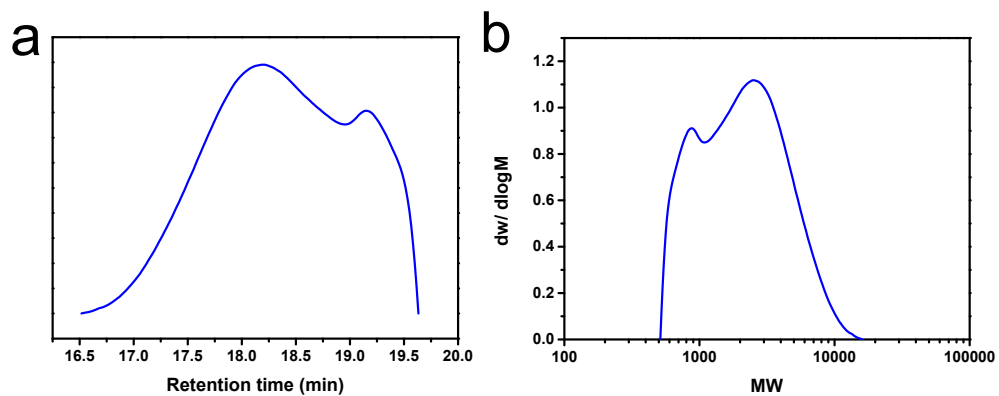


Fig. S1 (a) GPC curve and (b) molecular weight distribution curve of SBO.

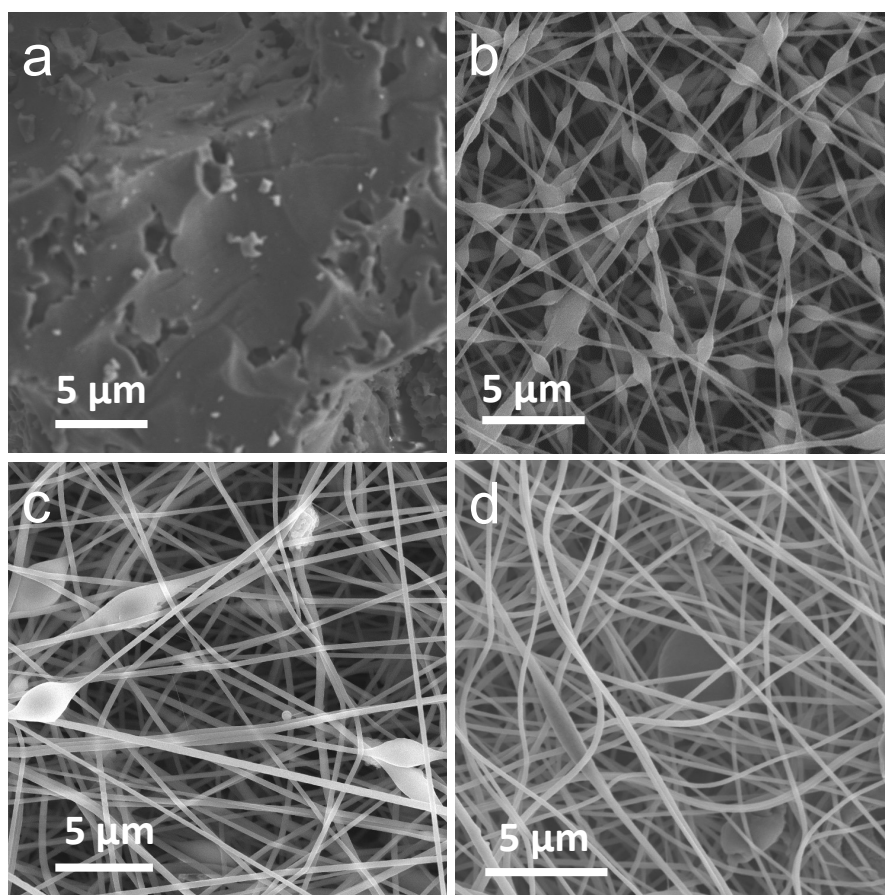


Fig. S2 Investigation of morphological evolution with the variation of the volume ratio between PAN/ DMF and SBO. SEM images of (a) SBO, (b) PNF-2, (c) PNF-1.7 and (d) PNF-1.3.

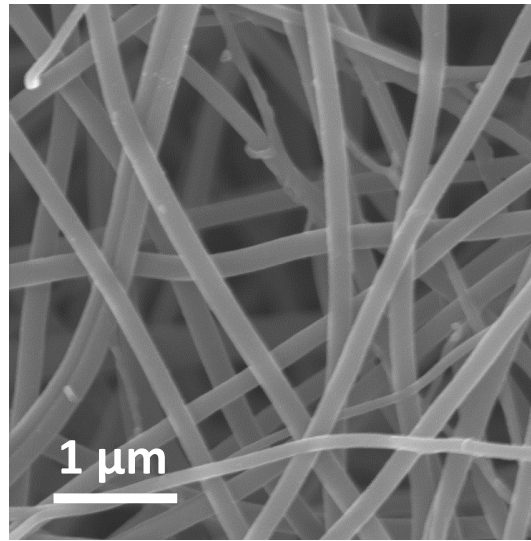


Fig. S3 SEM image of PAN.

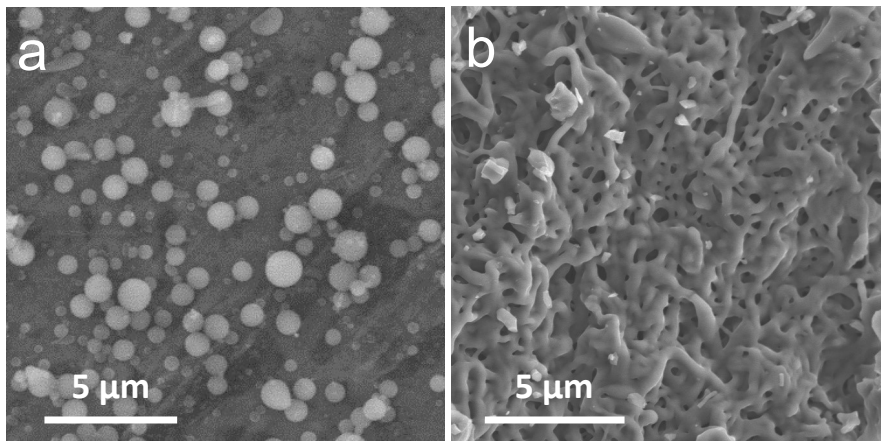


Fig. S4 SEM images of (a) control sample 1 with insufficient reaction time; (b) control sample 2 without crosslinking reaction at 200 °C.

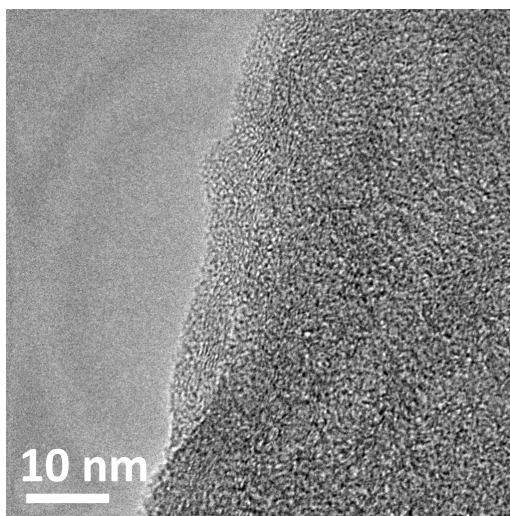


Fig. S5 TEM image of NPCNF.

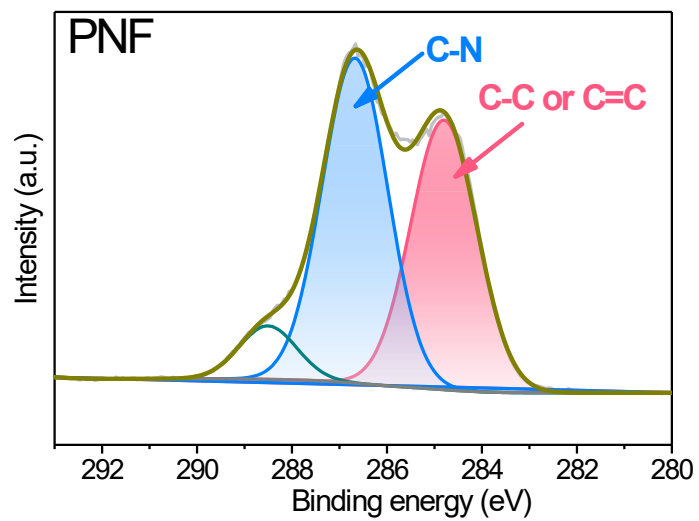


Fig. S6 The high-resolution XPS spectrum of C 1s of PNF.

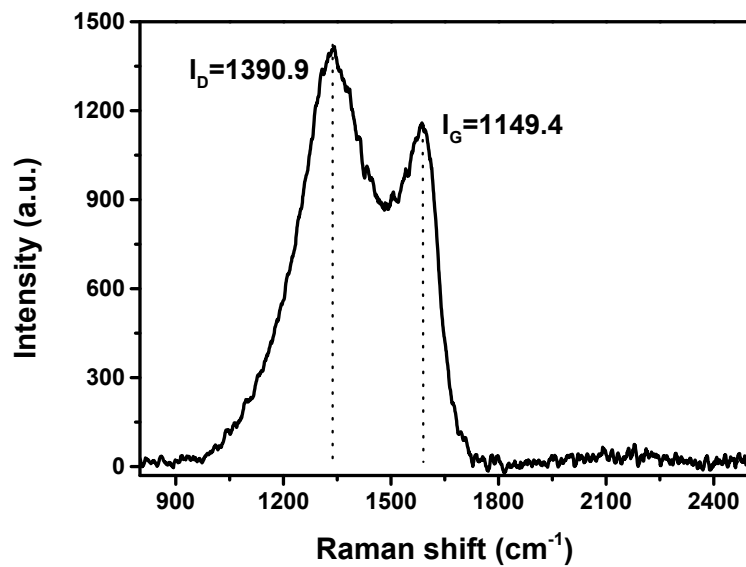


Fig. S7 Raman spectrum of NPCNF.

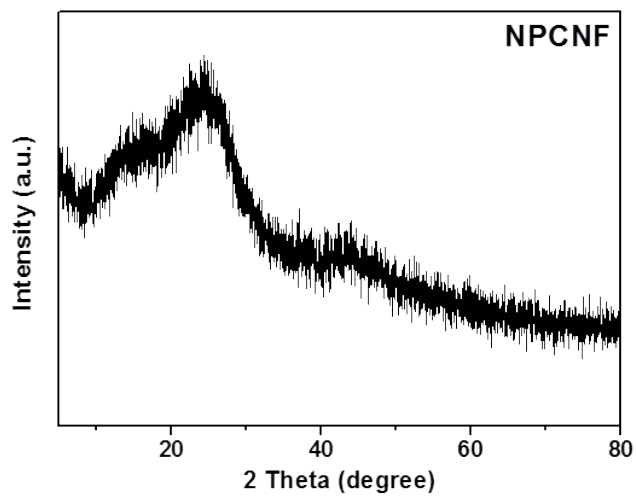


Fig. S8 XRD pattern of NPCNF.

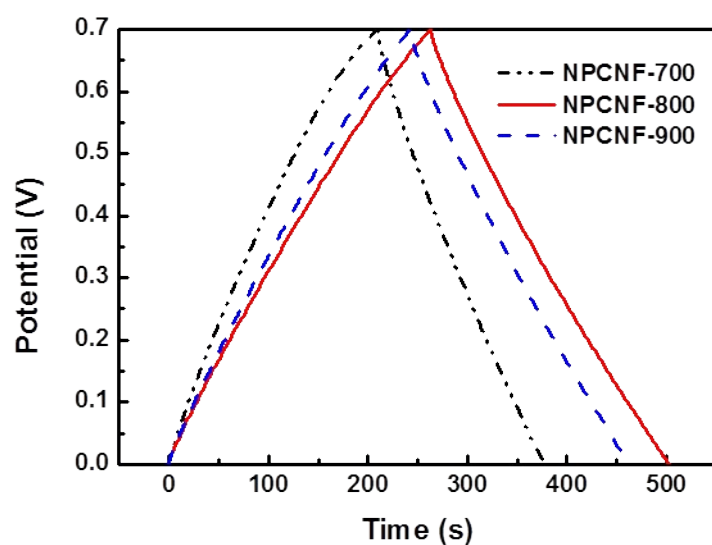


Fig. S9 Comparison of electrochemical performance of NPCNF-700, NPCNF and NPCNF-900 measured in a three-electrode system at 1 A g^{-1} .

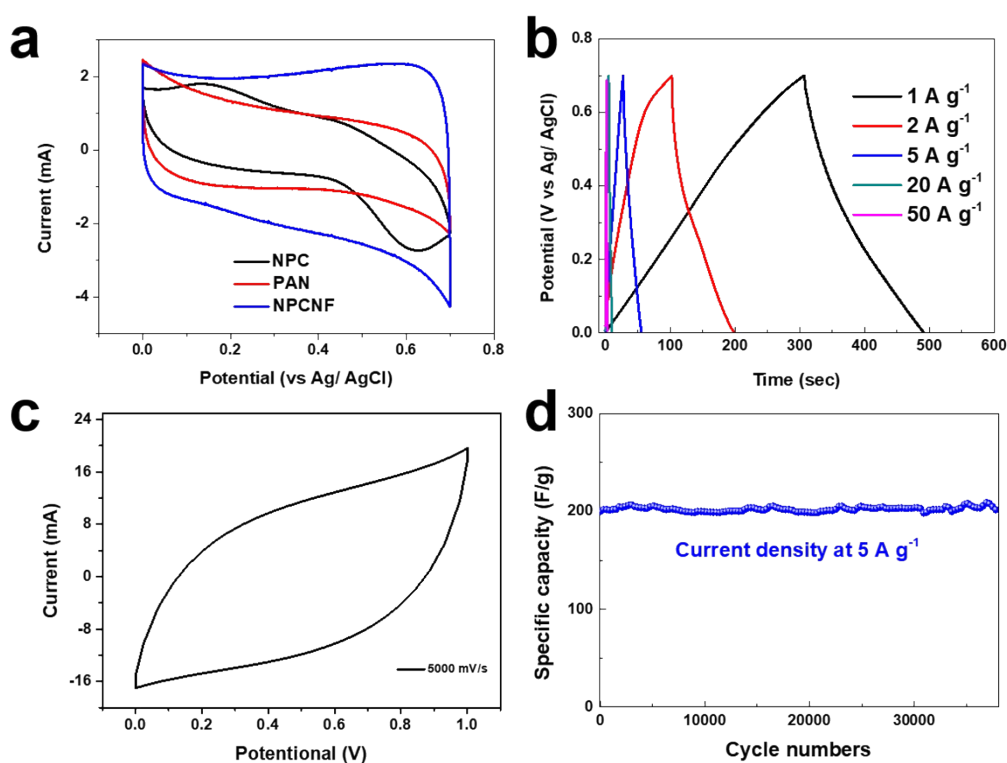


Fig. S10 Electrochemical capacitive performances of NPC, PAN and NPCNF electrodes: comparison of a) CV curves at a scan rate of 50 mV s^{-1} ; b) CV curve of NPCNF in 6 M KOH at 5000 mV s^{-1} ; c) galvanostatic charge/ discharge curves at different current densities; d) cycling stability at a current density of 5 A g^{-1} .

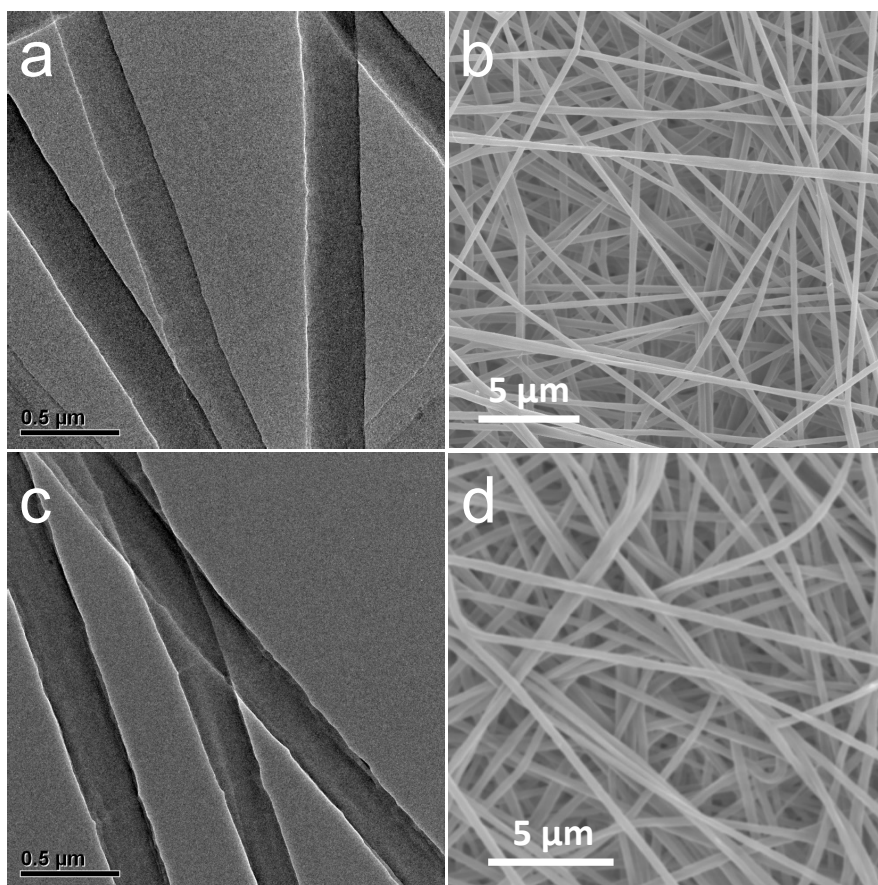


Fig. S11 (a) TEM image and (b) SEM image of the pristine NPCNF electrode; (c) TEM image and (d) SEM image of the NPCNF electrode after a galvanostatic charge-discharge process at 0.5 A g^{-1} for 200 cycles.

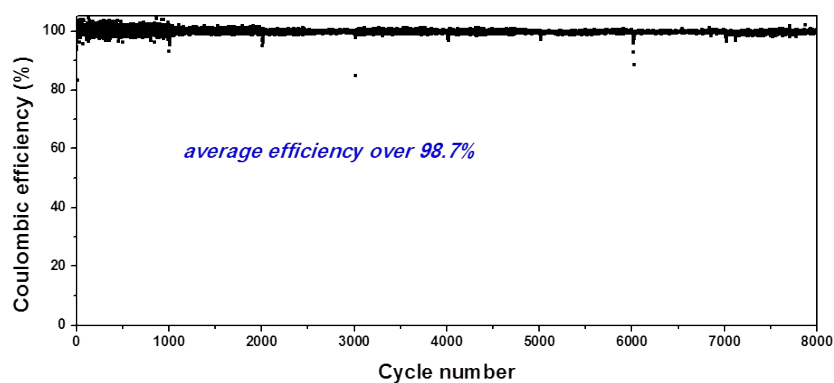


Fig. S12 Corresponding coulombic efficiency of NPCNF// AC LIC for 8,000 cycles at 5 A g^{-1} .